

---

### 3. Materials and Methods

#### Medicinal Plants in Contemporary Healthcare

Medicinal plants have taken an important role in human health, offering natural remedies for a wide range of ailments. They are having more bioactive compounds like alkaloids, flavonoids, terpenoids, phenols, etc., which exhibit therapeutic properties. Medicinal plants have been deeply valued across diverse cultures for their traditional healing practices, addressing conditions from common cold to chronic illnesses. The significance of such plants is vital for future biodiversity and supporting its sustainable healthcare practices. This approach also highlights their potential for alternative uses and underscores their significant therapeutic applications.

This division displays the materials and experimental methods adopted to develop and prove the anti-cancer efficacy of *Rhododendron arboreum* Sm. leaf and flower extracts against gastric cancer.

<b>PHASE I</b>		<b>Page No.</b>
3.1.	<b>Distribution and Taxonomical Features of <i>Rhododendron arboreum</i> Sm.</b>	67
3.1.1.	<b>Plant Classification and Description</b>	68
3.1.2.	<b>Ethnobotanical Uses of <i>R. arboreum</i></b>	69
3.1.3.	<b>Collection of Samples and Authentication</b>	69
3.1.4.	<b>Preparation of <i>R. arboreum</i> Sm. extracts</b>	70
3.1.5.	<b>Qualitative Phytochemical Analysis</b>	70
3.1.6.	<b>Quantitative Estimation of Phytochemical Constituents</b>	72
3.1.6.1.	Estimation of Total Flavonoid Content (TFC)	72
3.1.6.2.	Estimation of Total Tannin Content (TTNC)	
3.1.6.3.	Estimation of Total Alkaloid Content (TAC)	
3.1.6.4.	Estimation of Total Phenolic Content (TPC)	
3.2.	<b>Fourier Transform Infrared Spectroscopy (FT-IR)</b>	72
3.3.	<b>Nuclear Magnetic Resonance (NMR)</b>	73
3.4.	<b>Gas Chromatography-Mass Spectrometry (GC-MS)</b>	73
<b>PHASE II</b>		
3.5.	<b>Free Radical Scavenging Activity of <i>R. Arboreum</i> Leaves and Flower Extracts</b>	74-75
3.5.1.	DPPH Radical Scavenging Assay	
3.5.2.	ABTS (2,2'-azino-bis(3-ethylbenzothiazoline-6-sulfonic acid) Radicals	
3.5.3.	H <sub>2</sub> O <sub>2</sub> (Hydrogen Peroxide) Scavenging Activity	

3.5.4.	Lipid Peroxidation Inhibition Assay (LPO)	
3.5.5.	Ferric Reducing Antioxidant Power (FRAP)	
3.6.	<b>Toxicity Study- Brine Shrimp Lethality Assay</b>	75
3.7.	<b>Cytotoxicity Assay using AGS (Human Gastric Adenocarcinoma Cell-Line)</b>	75-77
3.7.1.	Cell Culture	
3.7.2.	Plant Extract Preparation	
3.7.3.	Cell Proliferation Assay	
3.8.	<b>Detection of Apoptosis using Flow Cytometer Analysis</b>	77
<b>PHASE III</b>		
3.9.	<b><i>In Vivo</i> Studies on Docetaxel-Induced Experimental Mice Model</b>	77
3.9.1.	<b>Standard Drugs</b>	78
3.9.2.	<b>Experimental Animals</b>	78
3.9.3.	<b>Dosage Regimen</b>	78
3.9.4.	<b>Tissue Sampling</b>	79
3.9.4.1.	<b>Preparation of Tissue Homogenate</b>	79
3.10.	<b>Estimation of Haematological Parameters</b>	79
3.10.1.	Enumeration of Red Blood Cells (RBCs)	
3.10.2.	Enumeration of White Blood Cells (WBCs)	
3.10.3.	Differential Leukocyte Count	
3.10.4.	Estimation of Haemoglobin: Sahil's Acid Haematin Method	
3.11.	<b>Estimation of Serum Biochemical Parameters</b>	80
3.11.1.	Determination of Total Proteins	
3.11.2.	Determination of SGOT and SGPT	
3.11.3.	Determination of Alkaline Phosphatase activity (ALP)	
3.11.4.	Determination of ACP	
3.12.	<b>Renal Function Parameters</b>	80
3.12.1.	Determination of Urea	
3.12.2.	Determination of Uric Acid	
3.12.3.	Determination of Creatinine	
3.13.	<b>Determination of Enzymatic and Non- Enzymatic Antioxidant Markers</b>	80-81
3.13.1.	Determination of Total Proteins	
3.13.2.	Determination of Superoxide Dismutase (SOD)	
3.13.3.	Determination of Catalase (CAT)	
3.13.4.	Determination of Glutathione Peroxidase (GPx)	
3.13.5.	Determination of Reduced Glutathione (GSH)	
3.13.6.	Determination of Lipid Peroxidation (LPO)	
3.14.	<b>Myeloperoxidase Activity (MPO)</b>	81-82
3.15.	<b>Histopathological Examinations</b>	82
3.16.	<b>Statistical Analysis</b>	82

PHASE IV		
3.17.	<b>In-silico ADME Studies by SwissADME</b>	82-83
3.17.1.	SwissADME	
3.17.2.	Chemical Structure and Bioavailability Radar	
3.18.	<b>Network Pharmacology</b>	83-84
3.18.1.	Compound Identification and Target Screening	
3.18.2.	PPI Network Construction and Key Gene Identification	
3.18.3.	Functional Enrichment and Pathway Analysis of <i>R. arboreum</i> in Gastric Cancer	
3.19.	<b>Molecular Docking</b>	85-86
3.19.1.	Protein Structure Acquisition and Ligand Preparation for Molecular Docking	
3.19.2.	Receptor Grid Generation	
3.19.3.	Molecular Docking using Schrodinger	
3.20.	<b>Molecular Dynamic Simulation (MDs)</b>	86-87

### 3.1. Distribution and Taxonomic Features of *Rhododendron arboreum* Sm.

*Rhododendron* species inhabit multiple forest types from lower subtropical to alpine elevations extending from the East to West of Himalayas. Approximately, 1025 *Rhododendron* species are present worldwide, among these 87 *Rhododendron* species exist in the Himalayas with six species unique to the Western Himalayan region. This genus establishes itself within different climatic conditions that occur in the steep rainforest zones (Dhyani *et al.*, 2023). The Himalayan region counts *R. arboreum* as a fundamental species because of its dual importance in medicine and ecological importance (Sharma *et al.*, 2020).

*Rhododendron arboreum* Sm. is a species of the Ericaceae family known for its medicinal properties. This plant species is distributed across various regions in India, spanning Arunachal Pradesh, Jammu and Kashmir, Manipur, Meghalaya, Mizoram, Nagaland, Sikkim, Uttarakhand, West Bengal and Himachal Pradesh (Mehta *et al.*, 2023).

### 3.1.1. Plant Classification and Description

Kingdom: Plantae

Class: Dicotyledonae

Sub-Class: Gamopetalae

Series: Heteromerae

Order: Ericales

Family: Ericaceae

Genus: *Rhododendron*

Species: *arboreum* Sm.

The name '*Rhododendron*' is derived from the Greek word 'Rhodon', denoting rose and 'dendron', denoting tree hence it is called the rose tree (Kumar *et al.*, 2020).

*Rhododendron arboreum* Sm. is an evergreen tree or large shrub that can grow up to 15-20 meters tall (Agarwal & Rajput, 2023). It is commonly called *Rhododendron* Tree (English), Lal Burnas (Hindi), Lali Gurans (Nepali) and Billi (Tamil). The leaves are leathery, oblong or lance-shaped, typically dark green on the upper surface and silvery or rusty-brown on the lower surface due to dense hairs. The plant is best known for its striking bell-shaped lowers (Figure. 5) which appear in clusters and range in colour from deep red to pink or white. Its bark is rough and dark brown and its branches spread broadly, giving it a rounded canopy.



**Figure 5.** Habit and Inflorescence of *Rhododendron arboreum* Sm.

### 3.1.2. Ethnobotanical Uses of *R. arboreum*

*Rhododendron arboreum*, is a significant plant in traditional medicine, food and cultural practices across various regions, particularly in the Himalayas. Fresh petals are prepared for sub-acidic jelly and sherbet (drink) popular market products for preventing altitude sickness among mountain climbers. However, it is advised to be cautious as consumption of large quantities of young leaves can lead to intoxication despite their medicinal applications, such as relieving headaches when applied to the forehead (Gautam *et al.*, 2020). In Nepali culture, the flowers are used for pickle preparation. The fresh or dried petals are also utilized for extracting fish bones when struck in the gullet. The wood serves as charcoal and fuel, its wood is crafted into items such as khukri handles, saddles, gift boxes, gunstocks and posts. Flowers and leaves are entwined on ropes for both house decorations and temple ornamentation (Ahmad *et al.*, 2022). Additionally, the plant plays a vital role in religious and cultural rituals, with its flowers being offered in temples and used during festivals (Srivastava, 2012).

### 3.1.3. Collection of Samples and Authentication

The leaves and flowers of *Rhododendron arboreum* Sm. were collected from Pedung village of West Kameng district of Arunachal Pradesh, India and authenticated at the BSI (Botanical Survey of India) Coimbatore, Tamil Nadu. (No.: BSI/SRC/5/23/2021/Tech on 25/02/2021) (Appendix I).

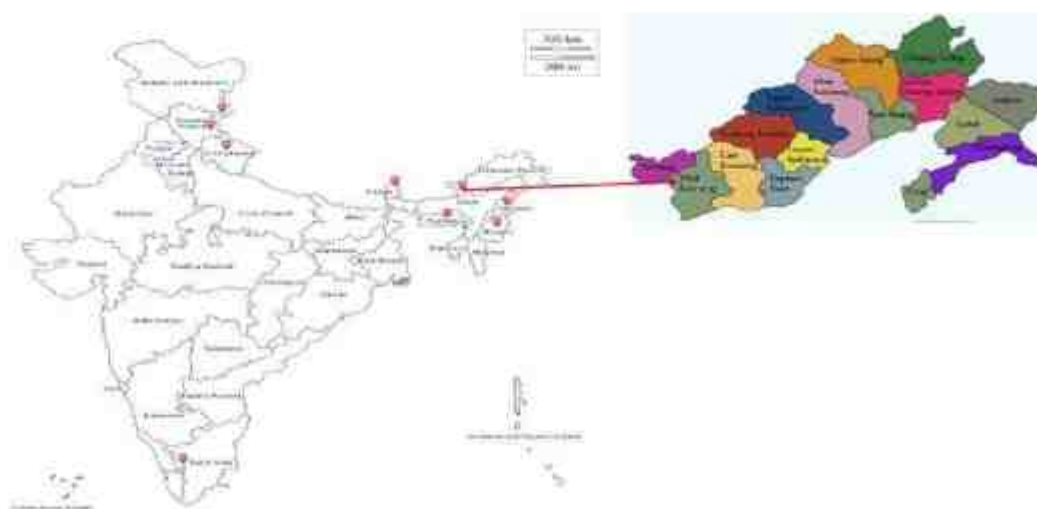


**Figure 6.** Distribution of *Rhododendron arboreum* Sm. in India (source: <https://in.pinterest.com/pin/616500636465514606/>)

### 3.1.4. Preparation of *R. arboreum* Sm. Extracts

The leaves and flowers were collected in January 2021, washed and dried in the shade for two weeks. The dried samples were then separately ground and stored in an airtight container for further studies.

For the preparation of extraction, 20 g of powdered leaves and 20 g of powdered flowers were taken in separate conical flasks and dissolved in 200 mL of different solvents (methanol, ethanol, chloroform, acetone, petroleum ether and distilled water). The conical flasks were then incubated in a shaker at 150 rpm for 48 hours. After incubation, the contents of each conical flask were filtered and the supernatant was collected and evaporated to obtain the concentrated extracts.

### 3.1.5. Qualitative Phytochemical Analysis

Preliminary phytochemical screening is the first measure in assessing the existence of a probable phytomedicine. These phytomedicines encompass various secondary metabolites including alkaloids, flavonoids, phenolics, terpenoids and glycosides each known for their potential health benefits. Phytochemical screening was done to assess the necessary tests for bioactive compounds using standard methods (Harborne, 1998; Pandey & Tripathi, 2014; Dhawan & Gupta, 2016; Abubakar & Haque, 2020).

**Table 1.** Preliminary Phytochemical Estimation of Phytoconstituents

S.no	Test	Reaction Mixture	Observation
1	Alkaloids- Mayer's Test	Plant extract + Mayer's reagent	Yellow precipitate formation indicates Alkaloids
2	Flavonoids- Alkaline Reagent Test	Plant extract + Sodium hydroxide (NaOH)	Intense yellow colour turning colourless with sulphuric acid indicates Flavonoids
3	Phytosterols- Salkowski's Test	Plant extract + Chloroform + Conc. Sulphuric acid	Golden yellow colour Indicates Phytosterols
4	Phenols- FeCl <sub>3</sub> Test	Plant extract + 2% of FeCl <sub>3</sub>	Blue, green or violet colour confirms the Presence
5	Tannins- FeCl <sub>3</sub> Test	Plant extract + 2% of FeCl <sub>3</sub>	Blue black or greenish black colour confirms the presence

6.	Diterpenes- Lieberman- Burchard's Test	Plant extract + chloroform + acetic anhydride + conc. H <sub>2</sub> SO <sub>4</sub>	Brown or red-coloured ring on sulphuric acid layer indicates presence
7.	Protein- Ninhydrin Test	Plant extract (1mL) + 0.2% Ninhydrin reagent, water bath for 5 minutes	Indication of blue, purple, violet colour confirms the presence of protein
8.	Amino acid- Ninhydrin Test	Plant extract (1mL) + 0.2% Ninhydrin reagent, water bath for 5 minutes	Purple or blue indicates their presence
9.	Carbohydrates - Molisch's Test	Plant extract + Alcoholic $\alpha$ -naphthol + Conc. Sulphuric acid	Violet colour at interface indicate carbohydrates
10.	Saponin (Foam) Test	Dil. plant extract + Shaken in graduated cylinder	Formation of 1cm foam layer indicates saponins
11.	Quinones- Ammonia Test	Plant extract + Dilute ammonia solution	Red, pink or purple colour indicates the presence
12.	Coumarins- FeCl <sub>3</sub> Test	Plant extract + 5% FeCl <sub>3</sub>	Green or blue colour confirms the presence
13.	Acidic Compounds	Plant extract + Sodium bicarbonate solution	Production of effervescence indicates acidic compounds
14.	Gallic acid	Matchstick + Plant extract + Conc. HCl	Red or pink colour in matchstick indicates presence
15.	Volatile Oils (NaOH)	Plant extract + Dil. Sodium hydroxide + Dil. HCl	White precipitate formation indicates presence
16.	Resins	Plant extract + Acetic anhydride + Conc. H <sub>2</sub> SO <sub>4</sub>	Orange to yellow colouration indicates presence
17.	Starch (Iodine Solution Test)	Plant extract + Iodine solution	Blue/black colour change indicates presence
18.	Carotenoids	Plant extract + 85% H <sub>2</sub> SO <sub>4</sub>	Blue colour at interface indicates the presence
19.	Oxalate	Plant extract + Glacial acetic acid	Greenish-black colour indicates the presence
20.	Vitamin C (DNPH test)	Plant extract + 2,4- dinitrophenylhydrazine + Conc. H <sub>2</sub> SO <sub>4</sub>	Yellow precipitate formation indicates Vitamin C

### **3.1.6. Quantitative Estimation of Phytochemical Constituents**

Ethnobotanical insights are integrated to understand cultural contexts and traditional knowledge associated with plant uses, guiding further analyses on bioactivity and potential therapeutic applications. Overall, this quantitative analysis lays a foundation for more advanced statistical testing and in-depth investigations into the pharmacological potentials of medicinal plants.

#### **3.1.6.1. Estimation of Total Flavonoid Content**

The total flavonoids content is expressed as milligrams of Rutin equivalents / gram using the method of Saeed *et al.*, 2012 ( Appendix II).

#### **3.1.6.2. Estimation of Total Tannin Content**

The quantification of total tannin content in the extracted plant samples was performed based on the method of Folin-Giocalteu, (1927) (Appendix III)

#### **3.1.6.3. Estimation of Total Alkaloid Content**

The determination of total alkaloid content by a simple spectrophotometric method (Yoshida *et al.*, 2010) (Appendix IV).

#### **3.1.6.4. Estimation of Total Phenolic Content**

The total phenolic content was quantified by the method of Chedea & Pop, 2019 ( Appendix V).

### **3.2. FT-IR: Fourier Transform Infrared Spectroscopy**

FT-IR relies upon the range of infrared light and a compound's chemical structure for this analytical process (Lorenz, 2020). FT-IR was performed on the methanol extracts of the leaf and flower in 100 mg KBr pellets as a consistent binder in the experimental tablets. A Shimadzu IR Affinity 1 (Japan) FT-IR was configured with the plant sample powdered, 400 to 4000  $\text{cm}^{-1}$  scanning range and 4  $\text{cm}^{-1}$  resolution. The results from FT-IR were used to assess and confirm the molecular composition and functional groups present in the plant extracts.

### 3.3. NMR: Nuclear Magnetic Resonance

The extracts were prepared by transferring 700  $\mu\text{L}$  of each sample into 5 mm NMR tubes for proton ( $^1\text{H}$ ) NMR analysis. Using a Bruker AVANCE III instrument operating at 600.13 MHz and 25°C,  $^1\text{H}$  NMR spectra were recorded with 16/64 scans, an acquisition time of 6.50 min per spectrum point and a 5 sec. relaxation delay. Signal suppression of  $\text{CD}_3\text{OD}$  and  $\text{D}_2\text{O}$  solvent signals was achieved through selective low-power irradiation at  $\text{H}_2\text{O}$  and  $\text{CH}_3\text{OH}$  frequencies during the reprocess delay. Free induction decays were Fourier transformed with  $\text{LB}=0$  Hz and spectra were processed for phase, baseline correction and calibrated to 0.0 ppm using Topspin software (version 3.2, Bruker). Internal standards included 3-(trimethylsilyl)-1-propanesulfonic acid (TSP) and triiodobenzoic acid (TBA) (Huang *et al.*, 2014).

Metabolite quantification using  $^1\text{H}$  NMR relies on the principle that signal intensity correlates with metabolite concentration. An internal standard (TSP or TBA) with a known mass is utilized to calculate the Intensity of the target metabolites using the equation:

$$m_x = m_{\text{ST}} * (A_x/A_{\text{ST}}) * (MW_x/MW_{\text{ST}}) * (N_{\text{ST}}/N_x)$$

Here,  $m_x$  represents the unknown mass of the target analyte,  $A_x$  and  $A_{\text{ST}}$  are the integral areas for the respective signals,  $N_x$  and  $N_{\text{ST}}$  denote the number of protons generating these signals and  $MW_x$  and  $MW_{\text{ST}}$  are the molecular weights of the target analyte and the internal standard (TSP/TBA) respectively. This method enables precise determination of metabolite concentrations based on their  $^1\text{H}$  NMR spectra and the calibration provided by the internal standard.

### 3.4. Gas Chromatography-Mass Spectrometry

Gas Chromatography- Mass spectrometry plays a key role in analysing unknown components of plants. GC-MS ionises compounds and calculate their mass number. Typical ionisation methods include CI (Chemical Ionisation) and EI (Electron Ionisation). The EI method offers positive outcomes in the compound quantification and is a precise-based method for disrupting components. In gas chromatography, the volatile components of a sample are separated using a suitable capillary column. Agilent GC-MS (CH-GCMSMS02)

used with 8890 GC and 7000 GC/TQ. Column: 30m long, 250µm diameter, 0.25µm film. Helium mobile phase, nitrogen collision gas. Solvent: methanol. Data analyzed via Mass Hunter. Temperature: 50-120°C at 5°C/min (16 mins), 120-210°C at 10°C/min (26 mins), 210-280°C at 10°C/min (38 mins). Scan range: 30-900 m/z (Tayade *et al.*, 2022).

The crude fraction was diluted with a suitable solvent (1/100, v/v) and filtered to remove particles. After preparation, 1 µL of the diluted crude extracts was injected using a syringe, with a 30:1 split ratio. Full-scan mass spectra were acquired across a specified scan range of 40–550 amu. The percentage composition of the components of the crude extract was determined by peak area analysis. The detection and characterisation of the molecular compounds in the crude extracts were performed by comparing gas-chromatography retention times and mass spectra with standard reference libraries.

Identification was achieved via comparison to the NIST database through GC-MS analysis. The spectra generated from the unknowns corresponded to the knowns in the NIST library via a match of retention time. Therefore, identification, molecular weight and chemical structure were established for the chemicals in the experimental samples.

### **3.5. Free Radical Scavenging Activity of *R. arboreum* Leaves and Flowers Extract**

#### **3.5.1. DPPH (2,2-Diphenyl-1-picrylhydrazyl) Radical Scavenging Assay**

The DPPH radical scavenging ability of the *R. arboreum* leaf and flower extracts was assessed based on the method described by BLOIS (1958) (Appendix VI).

#### **3.5.2. ABTS (2,2'-azino-bis(3-ethylbenzothiazoline-6-sulfonic acid)) Radical Scavenging Assay**

The ABTS radical cation decolourization assay was assessed based on the method described by Re *et al.*, 1999 (Appendix VII).

### 3.5.3. H<sub>2</sub>O<sub>2</sub> (Hydrogen Peroxide) Scavenging Activity

The ability of the leaf and flower extracts to scavenge hydrogen peroxide was assessed by the method of Ruch *et al.*, 1989 (Appendix VIII).

### 3.5.4. Lipid Peroxidation Assay (LPO)

The process by which free radicals steal electrons from lipids in the cell membrane, which results in cell damage, was assessed by the method of Repetto *et al.*, 2012 ( Appendix IX).

### 3.5.5. Ferric Reducing Antioxidant Power Assay (FRAP)

The antioxidant capacity of leaf and flower samples to reduce Fe<sup>3+</sup> to Fe<sup>2+</sup> were assessed by the method of Benzie & Strain, 1996 (Appendix X).

### 3.6. Toxicity Study- Brine Shrimp Lethality Assay

The powdered extracts of *Rhododendron* flower methanol (RFM) and leaves (RLM) were weighed and dissolved in saline water (1 mg/mL). The sample (RFM, RLM) of various volumes 100, 250, 500, 1000, 1500 µg/mL are introduced into each beaker containing 25 mL D.H<sub>2</sub>O respectively. In accordance with standard procedures by Hamidi *et al.*, 2014, the RFM and RLM extracts were used to conduct the brine shrimp lethality bioassay. A total of thirty shrimps were added to the sample solution of various concentrations and D.H<sub>2</sub>O served as blank and potassium dichromate (1 mg/mL) as a positive control respectively. The movement of brine shrimp was monitored at intervals of 1, 2, 4, 6, 24 hours and the mortality of shrimp was calculated. The mortality of the shrimps was monitored as that of blank and positive control.

### 3.7. Cytotoxicity Assay using AGS (Human Gastric Adenocarcinoma Cell-Line)

*In vitro* cell line studies involve cultivating cells in a controlled experimentation environment to investigate their behaviour under various conditions. These studies are important for examining the cellular responses to drugs, genetic modifications or other stimuli and understanding various disease mechanisms. By using immortalized cell lines such as AGS, studies assess

parameters like cell viability, proliferation and cell toxicity through assays like MTT. This approach delivers significant interpretation into the expected potency and mechanisms of new treatments contributing significantly to drug development and basic biological research.

### **3.7.1. Cell Culture**

The gastric adenocarcinoma cell-line (AGS) was obtained from the National Centre for Cell Science (NCCS), Pune. The cells were cultured and sustained in Ham's F-12 medium (HiMedia) supplemented with 10% Fetal Bovine Serum (FBS) (Gibco) and 1% penicillin-streptomycin (Gibco) following a standard protocol (Piletz *et al.*, 2018) and were maintained under 5% CO<sub>2</sub> incubator. Upon reaching confluency, cells were collected through trypsinization into a fresh complete medium (with serum and antibiotics) for subsequent parameter analysis. An aliquot of the collected cells was quantified using a hemocytometer. For the establishment of various exposure groups,  $1 \times 10^4$  cells were cultured overnight in a CO<sub>2</sub> incubator and sterile coverslips were inserted into each well for convenient cell handling prior to seeding.

### **3.7.2. Plant Extract Preparation**

The methanolic extracts of leaf and flower of *R. arboreum* (RLM & RFM) were concentrated using a rotary evaporator and dissolved in 0.1% DMSO, taking care that the final concentration of DMSO did not exceed 0.1% (v/v) to avoid interference with cell proliferation. The solution was then formulated in serum-free DMEM, filtered with a syringe filter (0.3 mm) and stored at 4°C for further studies.

### **3.7.3. Cell Proliferation Assay**

The 3-(4,5-dimethylthiazol-2-yl)-2,5-diphenyltetrazolium bromide (MTT) method was carried out according to the procedure described by Fan *et al.*, 2019.

Cell viability was evaluated using MTT assay, which relies on the reduction of MTT by the mitochondrial dehydrogenase enzyme in viable cells, resulting in a purple formazan product. Cells were plated in 96-well microplates ( $1 \times 10^4$  cells/well in 180  $\mu$ L medium) and cultured in a humidified

incubator at 37°C and 5% CO<sub>2</sub> for 24 hours. The DMSO extracts of *R. arboreum* were added in a serial concentration (125, 250, 500 and 1000 µl/mL) and incubated for a further 24 hours. The medium was then removed and 30 µl of MTT solution (5 mg/mL in PBS) was added to each well and incubated for 4 hours under dark conditions. After the unconverted MTT reagent was discarded, 1000 µl of DMSO was used to dissolve the formazan crystals. The formazan concentration was determined by measuring the absorbance at 540 nm using an ELISA reader.

### **3.8. Detection of Apoptosis using Flow Cytometer Analysis**

A FITC Annexin-V staining is preceded by the breakdown of membrane integrity that takes place during the last stages of cell death either as apoptosis or necrosis. The apoptotic activity of *R. arboreum* extracts towards AGS cells were determined by Annexin V-FITC/Propidium iodide binding assay. Concisely, the treated and control cells were rinsed with PBS and harvested by trypsin. Then the cells were added with 200 µL of trypsin-EDTA solution for 3-4 mins at 37°C. Subsequently, 5 µL of FITC, 5 µL of PI and 400 µL of 1X binding buffer was added to the cells and analysed using FACS BD cell quest Pro version 6.0. The cells positive for Annexin V and negative for PI were identified as early apoptotic cells and positive for PI and negative for Annexin V were identified as late apoptotic cells (Fan *et al.*, 2019).

### **3.9. *In vivo* Studies on Docetaxel-Induced Experimental Mice Model**

Mice as an *in vivo* model is vital for evaluating cancer treatment because it allows for evaluation within the constraints of the entire living creature that would not exist in a cultured cell experiment. Mice are either injected or bred genetically to get tumours, similar to what humans would have; thus, the evaluation of any new drug or treatment method occurs in relation to relative efficacy. This measurement involves determining end efficacy on growth, metastasis and subsequent quality of life for appropriate positive and negative outcomes or side effects. The mice models bridge the gap between *in vitro* findings and clinical applications, providing a practical platform for refining cancer therapies before human trials.

### 3.9.1. Standard Drugs

The standard drug docetaxel was acquired from Medicity Pharma (Batch No. : 36826), a local drug shop in Coimbatore, Tamil Nadu, India.

### 3.9.2. Experimental Animals

A group of 30 C57BL/6 mice, ranging in weight from 25 to 30 grams, were obtained from the animal house facilities at Biogen in Bangalore, India. The C57BL/6 mice were housed in polyethylene cages under controlled surroundings in aseptic habitat, with a twelve hours photoperiod cycle. They were supplied with standard-quality chow and access to water ad libitum. The experimental procedures on the rodents were approved by the Institutional Animal Ethics Committee (IAEC) of Avinashilingam Institute for Home Science and Higher Education for Women under project proposal number AIW: IAEC.2023:11. (Appendix XI). The gastric cancer was induced using  $1 \times 10^6$  AGS cells that were injected subcutaneously into the mice.

### 3.9.3. Dosage regimen

The rats were categorized into seven groups, each consisting of 4 individuals.

**Table 2.** Experimental Grouping and Treatment Protocol for *In vivo* Study

<b>Group I</b>	Served as the normal control and received a vehicle (DMSO).
<b>Group II</b>	Acted as the model group, receiving a subcutaneous injection of $1 \times 10^6$ AGS cells.
<b>Group III</b>	Received $1 \times 10^6$ AGS cells subcutaneously along with a standard drug (Docetaxel) at a dose of 10 mg/kg.
<b>Group IV &amp; V</b>	Received $1 \times 10^6$ AGS cells subcutaneously along with <i>R. arboreum</i> flower extracted with DMSO (RFD) at low (100 mg/kg) and high doses (200 mg/kg), respectively.
<b>Group VI &amp; VII</b>	Received $1 \times 10^6$ AGS cells subcutaneously along with <i>R. arboreum</i> leaf extracted with DMSO (RLD) at low (100 mg/kg) and high doses (200 mg/kg), respectively.

The plant samples were given to the mice groups IV to VII orally for 8 weeks. At the conclusion of the experiment, all the mice were acclimatized in the laboratory conditions. After specific treatment, the mice were sacrificed using chloroform.

#### **3.9.4. Tissue Sampling**

The abdomen were excised, opened along the convex border of the stomach, rinsed in 0.9% (w/v) NaCl and pinned flat on a silicone board for Petri dishes. Each stomach was digitally photographed; tumour characteristics were recorded on both the front and back sides of the stomach.

##### **3.9.4.1. Preparation of Tissue Homogenate**

The isolated stomachs were homogenised with a motor-driven, Teflon-coated homogeniser with 0.1 M Tris-HCl buffer (pH 7.4) to obtain a 10% homogenate. The homogenate was centrifuged at 10,000 rpm for 10 minutes at 5°C. The collected supernatant was used for further studies.

#### **3.10. Estimation of Haematological Parameters**

##### **3.10.1. Enumeration of Red Blood Cells (RBCs)**

The RBCs were assessed by the method of Raabe *et al.*, 2011 (Appendix XII (i))

##### **3.10.2. Enumeration of White Blood Cells (WBCs)**

The WBCs were determined by following the method of Gorva *et al.*, 2022 (Appendix XII (ii)).

##### **3.10.3. Differential Leukocyte Count**

The Leukocyte Count was determined using the method described by Nivedhita *et al.*, 2020 (Appendix XII (iii)).

##### **3.10.4. Estimation of Haemoglobin: Sahil's Acid Haematin Method**

The concentration of haemoglobin (Hb) was determined directly from the calibration tube and was assessed by the Sahil's method (Thakkar *et al.*, 2021) (Appendix XII (iv)).

### **3.11. Estimation of Serum Biochemical Parameters**

#### **3.11.1. Determination of Total Proteins**

Total Protein estimation was determined by the method of Waterborg *et al.*, 2009.(Appendix XIII (i) ).

#### **3.11.2. Determination of SGOT and SGPT**

The estimation of SGOT and SGPT in serum was determined by the method of Reitman & Frankel, 1957 (Appendix XIII (ii)).

#### **3.11.3. Determination of Alkaline Phosphatase activity (ALP)**

The ALP content was assessed enzymatically by the method of Marsh *et al.*, 1959 (Appendix XIII (iii))

#### **3.11.4. Determination of Acid Phosphatase (ACP)**

The ACP content was determined enzymatically by the method of Lin & Fishman, 1972 (Appendix XIII (iv)).

### **3.12. Renal Function Parameters**

#### **3.12.1. Determination of Urea**

The estimation of Urea was done by the method of Bergmeyer, 1965. (Appendix XIV (i))

#### **3.12.2. Determination of Uric Acid**

Estimation of Uric Acid was determined using the method of Holmes & Assimos, 2004 (Appendix XIV (ii)).

#### **3.12.3. Determination of Creatinine**

The estimation of Creatinine was determined through the method of Chaney & Marbach, 1962 (Appendix XIV (iii)).

### **3.13. Enzymatic and Non- Enzymatic Antioxidant Markers**

The enzymatic and non-enzymatic antioxidants markers reveal significant insights in cancer research. These includes enzymatic antioxidants such as catalase, superoxide dismutase and glutathione peroxidase, as well as non-enzymatic reduced glutathione. Lipid peroxidation occurs over time as free radicals are produced and lipids are stressed; therefore, measuring lipid

peroxidation relative to control is an effective way to determine the extent of oxidative stress applied to cells during treatment. In addition, measuring levels of antioxidants demonstrates the level of upregulation response to avoid further oxidative stress. Therefore, the response to increased damage either through stress or increased levels of antioxidants helps to acknowledge what is effective and what are the adverse effects and toxicities associated with cancer treatment.

#### **3.13.1. Determination of Total Proteins**

Total Protein was measured using the method of Waterborg *et al.*, 2009 (Appendix XV (i)).

#### **3.13.2. Determination of Superoxide Dismutase (SOD)**

The determination of SOD was based on the method of Kakkar *et al.*, 1984 (Appendix XV (ii))

#### **3.13.3. Determination of Catalase (CAT)**

The determination of CAT was assessed according to the method of Sinha *et al.*, 2022 (Appendix XV (iii)).

#### **3.13.4. Determination of Glutathione Peroxidase (GPx)**

The GPx were determined by the method of Rotruck *et al.*, 1973 (Appendix XV (iv))

#### **3.13.5. Determination of Reduced Glutathione (GSH)**

Determination of GSH was evaluated using the method of Ellman, 1959 (Appendix XV (v)).

#### **3.13.6. Determination of Lipid Peroxidation (LPO)**

The LPO was determined according to the method of Okhawa *et al.*, 1979 (Appendix XV (vi))

#### **3.14. Myeloperoxidase Activity (MPO)**

Myeloperoxidase activity was measured using the method outlined by Wei and Frenkel, 1991.

## Procedure

Tissue samples were homogenized in 5 mL of hexadecyltrimethylammonium bromide prepared in a 50 mM potassium phosphate buffer (pH 6.0). The resulting homogenate was centrifuged at 10,000 rpm for 20 minutes. To each tube, 1.3 mL of 25 mM 4-aminoantipyrine- 2% phenol solution along with 1.5 mL of 1.7 mM H<sub>2</sub>O<sub>2</sub> were added and equilibrated for 3-4 minutes 525 nm.

### 3.15. Histopathological Examinations

The pancreas and liver was cut out, excised and rinsed in an ice-cold saline solution. A portion of the tissues was fixed in a 10% neutral formalin fixative solution, dehydrated in alcohol and then embedded in paraffin. Thin sections (4–5 µm) were prepared using a rotary microtome and stained with hematoxylin and eosin (H&E) dye to examine histopathological changes (Ahmed *et al.*, 2015).

### 3.16. Statistical Analysis

Statistical analyses were performed in triplicate to ensure accuracy and the findings were presented as mean values accompanied by their standard deviations. Subsequently, IC<sub>50</sub> values for the antioxidant assays were calculated using the linear regression method. The experimental data underwent analysis using one-way factorial ANOVA, followed by the Tukey multiple range test at  $\alpha = 0.05$ . The experimental data for animal study were depicted as mean  $\pm$  standard deviation from a one-way ANOVA followed by Dunnett's test (n=6). Mean values are shown as  $\pm$  SEM.

### 3.17. *In silico* Studies ADME using SwissADME Tool

#### 3.17.1. SwissADME

To serve as an effective drug, the ligand molecule should reach the diseased protein target in the body in adequate concentration and remain in an active state for a long time for the anticipated biological events to follow. SwissADME was used for estimating the ADME behaviours of each compound. SwissADME is a web tool that provides free access to a collection of rapid and predictive models for physicochemical parameters, pharmacokinetics and

drug-likeness and medicinal chemistry among which proficient methods such as the BOILED-EGG, iLogP and Bioavailability Radar. ADME means absorption, distribution, metabolism and elimination. It was conducted via an intuitive interface accessible through the login website <http://www.swissadme.ch>.

### **3.17.2. Structure and Bioavailability Radar**

The drug likeness of desired molecules can be accessed with bioavailability radar which provides initial glance. The present work deals with various physicochemical properties like molecular size, flex (NRotB flexibility), polar (TPSA Polarity), lipo (Lipophilicity), H-bond acceptors, H-bond donors, Gastro-Intestinal absorption, Blood Brain Barrier Permeation, CYP2D6 inhibitor, Lipinski violations (Lipinski *et al.*, 2012) and PAINS alerts. Presented in Appendix XVI.

### **3.18. Network Pharmacology**

#### **3.18.1. Compound Identification and Target Screening**

The main chemical compounds of *Rhododendron arboreum* leaves and flowers were identified employing data from GC-MS analysis and the IMPPAT 2.0 database (<https://cb.imsc.res.in/imppat/>). The key active bioactive compounds were selected based on a drug-likeness (DL) threshold value of  $\geq 0.18$ . The targets connected with these components were regained from the IMPPAT 2.0 database, the Therapeutic Targets Database (TTD, <https://bidd.nus.edu.sg/group/ttd/ttd.asp>) and further cross-referenced with BindingDB (<https://www.bindingdb.org/rwd/bind/chemsearch/marvin/FMCT.jsp>). Each candidate target was then input into the UniProt database (<https://www.uniprot.org/>) to identify human genes linked to these targets, specifically focusing on the species *Homo sapiens*. Additionally, human genes associated with gastric cancer were obtained from the GeneCards database (<https://www.genecards.org/>) and DisGeNET database (<https://disgenet.com>). Finally, the potential targets of *Rhododendron arboreum* against gastric cancer were identified by intersecting the above targets using the Venn diagram tool (<https://bioinfogp.cnb.csic.es/tools/venny/index.html>).

### 3.18.2. PPI Network Construction and Key Gene Identification

PPI (Protein-Protein Interaction) data were acquired from STRING v11.0 (<https://string-db.org/>) and transformed using the UniProt information database to eliminate redundant items and merge data to obtain gene symbols. These gene symbols were searched using the multiple proteins option in STRING, with the organism designated as *Homo sapiens* and the required interaction score was configured to be greater than 0.4. The resulting PPI network, linking compound target symbols with gastric cancer-related target symbols was then visualized using Cytoscape 3.6.1 software (<https://cytoscape.org/>). Key genes within the network were identified using the cytoHubba plugin, selecting genes with a degree exceeding twice the median value and the top 10 (ESR1, GSK3B, ESR2, CYP19A1, MET, HMGCR, KDR, IGF1R, MMP9 and EGFR) most relevant genes were chosen for further analysis.

### 3.18.3. Functional Enrichment and Pathway Analysis of *R. arboreum* in Gastric Cancer

The ShinyGO 0.80 tool (<http://bioinformatics.sdstate.edu/go/>) was utilized for clustering and functional enrichment exploration of the targets of active compounds resistance to gastric cancer. This exploration was performed through examining GO and KEGG pathways using the DAVID (Database for Annotation, Visualization and Integrated Discovery) database (<https://david.ncifcrf.gov>). DAVID serves as a web-based portal offering biologists a complete resource for systematic dataset analysis including gene annotation, GO and KEGG pathway enrichment analysis. Pathway enrichment for accepted proteins with a p-value > 0.01 was considered significant. The biological processes and pathways with the most significant p-values were highlighted based on the results obtained with DAVID and ShinyGO 0.80. The results of the KEGG enrichment analysis were used to construct a KEGG pathway network to identify the proteins involved in the effects of *R. arboreum*. In addition, the STRING results were used to map the gene pathway of *R. arboreum* against gastric cancer, visualise the biological pathways and the main targets involved and investigate the potential mechanisms of *R. arboreum* in combating gastric cancer.

### 3.19. Molecular Docking

#### 3.19.1. Protein Structure Acquisition and Ligand Preparation for Molecular Docking

The 3D structures of the target proteins were downloaded from the RCSB PDB database (<https://www.rcsb.org/>) with the organism source set to *Homo sapiens* and refined at resolutions ranging from 2.0 to 3.0 Å. Active compounds were obtained from the PubChem (<https://pubchem.ncbi.nlm.nih.gov>) and ChEMBL databases (<https://www.ebi.ac.uk/chembl/>) to be used as ligands. Ligand preparation involved estimating partial atomic charges using the OPLS-3 force field while preserving chirality and generating up to 64 low-energy stereoisomers per ligand. This was followed by geometry and energy minimization. The prepared ligands were then subjected to molecular docking using the Glide module within the Schrödinger suite. The selection of ligands was based on their binding energies with the target protein. Post-docking analysis was conducted to examine the interactions between the selected ligands and the target protein, focusing on those with favorable interaction profiles. This thorough selection process identified potent ligands from *R. arboreum*, laying the preliminary work for further experimental validation and potential therapeutic development against gastric cancer.

Target proteins (ESR1, GSK3B, KDR, IGF1R, MM9P and EGFR) were generated through the Protein Preparation Wizard of the Schrodinger Suite. The target protein structure was uploaded and processed, bond order was assigned, and hydrogens were added to avoid hydrogen overlapping. Crystallographic waters further than 5 Å away from hetero groups were removed. Ultimately, missing side chains and loops were filled in and protonation states were adjusted to 7.0 to ensure a neutral pH of the biological environment; restrained energy minimization was ultimately performed so that any steric clashes would be alleviated and geometry would be enhanced for accurate docking with compounds from *R. arboreum*.

### 3.19.2. Receptor Grid Generation

The virtual receptor grid of the target protein in the Schrödinger suite was generated with the expected binding site from the co-crystallized ligand. As previously established, the region of the co-crystallized ligand was found by identifying the center of the active site and creating the binding pocket afterward. A grid box was set to encompass the active site and all the necessary pockets for ligand interaction as the binding region. *Van der Waals* scaling and charged restrictions were set to default to allow for proper positioning adjustments of the receptor. Therefore, this reconstruction of the generated binding pocket from the crystal structure allowed for proper, effective virtual hits vs. docking of *R. arboreum* compounds to gastric cancer.

### 3.19.3. Molecular Docking Using Schrödinger

Molecular docking of target proteins with *R. arboreum* significant phytoconstituents was performed using the Glide module of the Schrödinger suite. A receptor grid was generated for the processed target proteins (ESR1, GSK3B, KDR, IGF1R, MM9P and EGFR), ensuring docking occurs in a fixed location. The ligands were then docked subsequently based upon predicted binding affinities with respective ligand binding sites. Standard Precision (SP) docking was applied to render the best results without over taxing of computational resources. Following docking, ligand binding were assessed for significant interactions (hydrogen bonds, hydrophobic interactions and  $\pi$ - $\pi$  stacking) relegated to active site confines. Therefore, molecular docking provided insights into which compounds had the ability to act as inhibitors for further downstream wet lab studies for gastric cancer. Similarly, the study was also carried out with the comparison of standard drug-docetaxel.

### 3.20. Molecular Dynamic simulation (MDs)

Molecular Dynamic simulates the movement of proteins and ligands by observing it in real time via the Molecular Dynamics Environment (Biswas *et al.*, 2023). The goal of MDs is to determine what ligand and protein do in the natural state while simultaneously measuring the movement of protein-ligand complexes in a simulated environment with biochemical factors present (Bhunia *et al.*, 2021). The MDs was performed by Desmond Software

version 7.3, which operates within Maestro including the RMSD, RMSF and ligand properties.

The deposited protein-ligand complexes were introduced to the orthorhombic cubic solvent box via System Builder in Desmond, where TIP4P interaction sites were applied, creating 10 Å buffers around the proteins from the edges of the solvent box. The study chose a specific representation solvent model TIP4P, which has four interaction sites to more effectively simulate liquid water during the run of simulation (Kadaoluwa, 2021). The minimization calculations for equilibration were conducted with 21 Cl ions, 0.15 M NaCl with the OPLS4 force field (Wu *et al.*, 2023). The equilibration took place with an NPT ensemble at 300K and 1.01325 bar pressure. MDs ran 1000 distinct trajectories of 100 ns each to see if the protein-ligand remained stable by the end of the simulation.